forests

MDPI

Article

Modeling Climatic Influences on Three Parasitoids of Low-Density Spruce Budworm Populations. Part 3: *Actia interrupta* (Diptera: Tachinidae)

Jacques Régnière *, Jean-Claude Thireau, Rémi Saint-Amant and Véronique Martel

Canadian Forest Service, Natural Resources Canada, P.O. Box 10380, Stn. Ste-Foy, Quebec, QC G1V 4C7, Canada; cthireau@hotmail.com (J.-C.T.); remi.saint-amant@nrcan-rncan.gc.ca (R.S.-A.); veronique.martel@nrcan-rncan.gc.ca (V.M.)

* Correspondence: jacques.regniere@nrcan-rncan.gc.ca

Abstract: This article is the third and last of a series of models developed to investigate the impact of climate on the spatiotemporal biology of parasitoids. After two earlier papers investigating *Tranosema rostrale* and *Meteorus trachynotus*, this last article concerns the tachinid fly *Actia interrupta* (Diptera: Tachinidae). An individual-based model of the seasonal biology of *A. interrupta* was developed to determine the impact of climate on its interactions with two of its hosts, the spruce budworm *Choristoneura fumiferana* (Lepidoptera: Tortricidae) and the obliquebanded leafroller *C. rosaceana* in eastern North America. The model is based on the developmental responses of 'the parasitoid's successive life stages and the ovipositional response of adult females to temperature. It was found that the number of generations this parasitoid undergoes each year varies geographically from two to four, and that its potential growth rate, as dictated by synchrony with larvae of its overwintering host *C. rosaceana*, is highly patterned geographically and topographically as a result of phenological matching with larvae of obliquebanded leafroller entering diapause in late summer.

Keywords: biodiversity; ecology; environment; forest; global change; insect; parasitoids; spruce budworm; seasonal biology; host synchrony

check for updates

Citation: Régnière, J.; Thireau, J.-C.; Saint-Amant, R.; Martel, V. Modeling Climatic Influences on Three Parasitoids of Low-Density Spruce Budworm Populations. Part 3: *Actia interrupta* (Diptera: Tachinidae). *Forests* **2021**, *12*, 1471. https://doi.org/10.3390/f12111471

Academic Editors: Jakub Horák and Adam Véle

Received: 4 October 2021
Accepted: 26 October 2021
Published: 28 October 2021

Publisher's Note: MDPI stays neutral with regard to jurisdictional claims in published maps and institutional affiliations.

Copyright: © 2021 by the authors. Licensee MDPI, Basel, Switzerland. This article is an open access article distributed under the terms and conditions of the Creative Commons Attribution (CC BY) license (https://creativecommons.org/licenses/by/4.0/).

1. Introduction

Climate change threatens ecosystems in a variety of ways [1]. Changes in the distribution and demographic behavior of herbivorous insect populations are particularly feared [2]. Understanding outbreaks or eruptive events has always been of great interest and challenge, be it in the context of human health [3] or insect pests [4]. Many biotic and abiotic factors influence the development and spread of outbreaks, and complex interactions are at play. Insect development is directly influenced by daily temperature fluctuations, and their distribution is influenced by local climate and therefore by climate change [5]. While it is relatively easy to quantify the direct impact of temperature on the different life stages of insects in the laboratory [6–8], temperature is not the only important factor. Ecological interactions with other organisms (host trees, natural enemies, competitors) play an important role [9,10]. The influence of climate on predator−prey interactions is profound, and can affect the ability of natural enemies to regulate their prey populations [11,12]. Mechanistic individual-based models are powerful tools to address such complex issues at the population level [13].

Spruce budworm, *Choristoneura fumiferana* (Clemens) (Lepidoptera: Tortricidae; SBW) is one of most important forest pests in North America [14]. Outbreak cycles occur at intervals of 30–40 years [15,16]. During the different stages of the outbreak, larvae are attacked by a diverse community of parasitoids constituting a complex and dynamic food web [17]. The importance of various members of this web varies in time [18], depending on the phase of the outbreak cycle, as well as in space, most probably depending on local climate.

This is the last of a series of three papers where we explore with individual-based models the effect of temperature on the seasonal interactions between parasitoids and their insect hosts. In the first paper, we developed the general approach using the ichneumonid larval parasitoid *Tranosema rostrale* (Brischke) (Hymenoptera: Ichneumonidae) in interaction with two main host tortricids, the spruce budworm, *C. fumiferana* and the obliquebanded leafroller (OBL), *C. rosaceana* (Harris) [19]. In the second paper, we did a similar analysis for the interaction of the braconid wasp *Meteorus trachynotus* (Viereck) (Hymenoptera: Braconidae) interacting with the same two tortricid hosts [20].

Here, we develop a seasonality model for the tachinid fly *Actia interrupta* Curran (Diptera: Tachinidae), again with the SBW and OBL as hosts. *A. interrupta* is a common parasitoid of late instar of these two tortricids. It has a wide host range that includes mostly tortricid larvae, many belonging to well-known forest pest genera, such as *Acleris*, *Archippus*, *Archips* and *Choristoneura* [21,22]. Among these hosts species, two other than SBW and OBL are often abundant in eastern conifer forests for North America: the black-headed budworm *Acleris variana* (Fernald), and the large aspen tortrix *Choristoneura conflictana* (Walker). In experiments that will be reported elsewhere, we have found that *A. interrupta* successfully overwinters inside diapausing third instar OBL larvae, not as a pupa. *A. variana* is univoltine, and enters overwintering diapause in the egg stage in mid-July. Therefore, it cannot be an overwintering host for this parasitoid. *C. conflictana* is also univoltine and enters diapause in the first instar in late July, after briefly feeding on deciduous leaves. It could conceivably be an overwintering host for the parasitoid, if *A. interrupta* indeed attacks such small larvae. However, very little is known about the thermal responses of *C. conflictana* and this species' seasonality cannot currently be modeled.

The thermal responses of SBW and OBL are known, and detailed phenology models are available for both species [19,23]. However, little is known about the seasonal biology and ecology of *A. interrupta*, other than the fact that its impact increases greatly following the collapse of SBW outbreaks, and that it is one of the few parasitoid species found during the endemic phase between two outbreaks [24]. The female deposits larvae on foliage near host feeding sites, and the task of host finding is left to the young maggot [25] that penetrates the host through the thin intersegmental integument of the abdomen or thorax. At the end of the third instar, the maggot egresses from its host, and forms an easily recognizable puparium, usually in the silk webbing of the host's feeding site.

The goal of the model discussed here is not to simulate the impact of the parasitoid on host populations, but rather to evaluate the impact of temperature and host availability on the parasitoid's performance. We use this model to map the potential performance of the parasitoid under the current and future climate in eastern North America, where SBW causes most of its economic damage to conifer forests.

2. Materials and Methods

2.1. Experimental Data

Field observations of the attack rates by adult *A. interrupta* on SBW host larvae were obtained from two locations, described in detail in [26]: near Armagh, Quebec (47.7667° N, 70.6575° W, 277 m), between 1987 and 2018, and near Petit Lac à l'Epaule, QC (47.2997° N, 71.1939° W, 789 m, hereafter Epaule) between 1989 and 2018. Because SBW populations were too low for sampling wild larvae from host foliage, attack rates by the parasitoid were measured by a sentinel method [27]. Briefly, sentinels are laboratory-reared insects that are placed at intervals of 3–4 d on host trees in the field for 7 d exposure periods, recovered and reared to diagnose the presence of parasitoids. At Epaule, *A. interrupta* was recovered from sentinel larvae in only 16 of those 30 years, and at much lower frequencies than in Armagh.

The data available on the overwintering of *Actia interrupta* in larvae of the OBL, the thermal responses of immature stages, adult reproduction and longevity were obtained under controlled laboratory conditions using either wild or laboratory-reared parasitoids.

Because of their complex nature, the methods and results of these experiments will be reported in detail in an upcoming paper.

2.2. Analysis

Three sets of *A. interrupta* individual development times at a range of constant temperature were used: (1) overwintered maggot inside its overwintering host, *C. rosaceana*, (2) in the puparium and (3) inside the summer larval host. While the latter measurements were made using fifth instar spruce budworm as hosts, we assume that maggot development times are the same in the non-diapausing (summer) OBL host as in SBW.

The relationship between development rate r (d^{-1}) and temperature T (°C) in the three datasets was described with the equation of [6]:

$$r = \begin{cases} \varphi\left[e^{\omega(T-T_b)} - \left(\frac{T_m-T}{T_m-T_b}\right)e^{-\omega(T-T_b)/\Delta_b} - \left(\frac{T-T_b}{T_m-T_b}\right)e^{\omega(T_m-T_b)-(T_m-T)/\Delta_m}\right]\varepsilon \text{ for } T_b \le T \le T_m \\ 0 \text{ otherwise} \end{cases} \quad (1)$$

where φ, ω, T_b, T_m, Δ_b and Δ_m are parameters to be estimated, and ε is a lognormally distributed random number with mean 1 and standard deviation σ_ε, a parameter that is also estimated from data. Because low-temperature experimental treatments were not available, the value of the lower threshold temperature T_b was fixed to 0. All other parameters of Equation (1) (φ, ω, T_m, Δ_b, Δ_m and σ_ε) were estimated using the Excel Solver, by maximum-likelihood [6]. Procedure NLMIXED of SAS/9.1 was used to obtain standard errors of the parameter estimates.

2.3. Model Description

The model (Figure 1), coded in C^{++}, runs under BioSIM [28]. The simulation starts with 100 individual maggots overwintering in diapausing OBL hosts. It inputs daily minimum and maximum air temperature, from 1 January, and outputs daily the frequency of *A. interrupta* maggots (active or in diapause), puparia, and adults in each successive generation, as well as the frequency of larvae of both SBW and OBL hosts, obtained from existing models of their respective seasonality [19,23]. In the model, an *A. interrupta* maggot enters diapause as soon as its OBL host larva does (which occurs when the latter molts to the third instar, after having been induced into diapause by short daylength (<13.5 h) during either the first or the early half of the second instar [29].

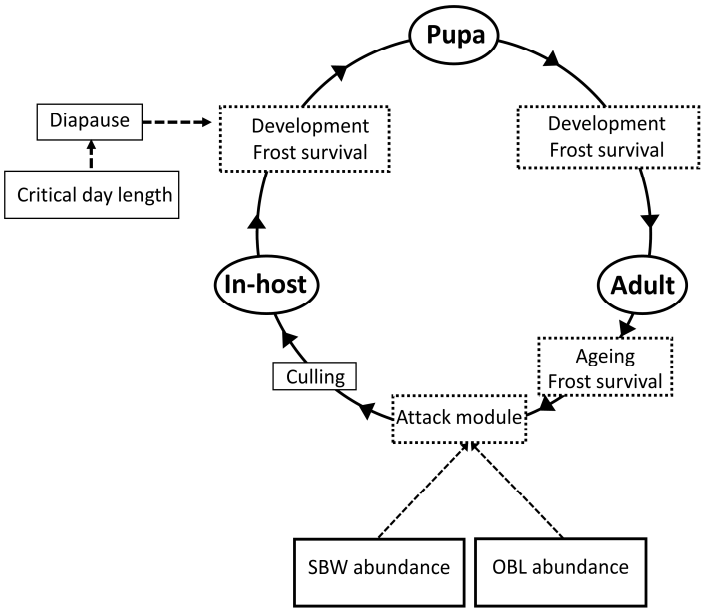

Figure 1. Flow chart of the model linking the parasitoid *Actia interrupta* to larvae of its two hosts, SBW and OBL. Models of SBW and OBL abundance are described in [19,23].

Longevity is an individual constant that averages 22.4 days, drawn from the lognormal distribution with mean 2.973 and standard deviation 0.552. Because we lack information on a relationship between larviposition and age, we assume that females distribute their reproductive output evenly throughout their reproductive lives. An individual's fecundity is drawn from a normal distribution with mean 129.4 and standard deviation 47.2 eggs per female. The process of larviposition starts after a 5-day pre-larviposition period during which eggs develop then hatch inside the adult females.

To make the model responsive to host density (and thus to synchrony), we included an attack module developed to study the seasonal biology of *Tranosema rostrale* [19]. This module consists of a combination of models that simulate the development of SBW and of OBL, coupled to the adult parasitoid by a theoretical numerical response relationship [30]:

$$N_a = \frac{aN_h\Delta t}{1 + at_hN_h} \quad (2)$$

where N_a is the number of hosts attacked per time step (Δt = 0.1667 or 4 h), N_h is the number of hosts available (larvae of SBW and OBL), a is the area of discovery, and t_h is the proportion of a time step spent attacking a host once it has been found. Values of a = 0.3 and t_h = 0.7 were used, because they produce a realistic response ranging from 0 to 1.25 attacks per time step as N_h increases from 0 to 200, the maximum number of host larvae available at any given time in our model (100 each for SBW and OBL). The attack module assumes that all hosts in the larval stage are available to be attacked by any given parasitoid adult. The maximum potential fecundity of *A. interrupta* in this model is 7.4 maggots per day, or 1.23 maggots per 4 h (the time step in our model). Maggots that are not deposited by a female remain available in the next time step. Because hosts are rarely both at full abundance, this functional response results in reduced parasitoid realized fecundity. It ensures that overlap between *A. interrupta* adult abundance and the availability of host larvae becomes a factor determining annual population growth rate, without consideration of the relative density of the three species.

Because the model makes no use of male *A. interrupta*, all individuals are assumed to be females. To balance population growth rates, a constant culling rate (κ = 97.96%) is applied to the creation of new maggot individuals in all generations. This number was arrived at by adjusting κ so that the average predicted annual population growth rate in Armagh and at Epaule averaged 1.0 over the period 1986–2019, reasoning that because the parasitoid is present (and expected to be persistent) in those two locations, its population growth rate probably averages near 1, overall (otherwise, the species would go extinct or become exceedingly abundant). The only other source of mortality in the model is death of the host larva from frost, which occurs whenever an individual SBW or OBL not in diapause is exposed to a temperature < 5 °C (after [19]).

2.4. Simulations

The methods used here are very similar to those used in [19,23] and are summarily described here. For any given simulation location (specified by its latitude, longitude and elevation), the BioSIM software [28] matches the four nearest weather stations from a database compiled from every available North American source of daily minimum and maximum air temperature records. It then applies regional gradients based on the 60 nearest stations to adjust for differences in elevation, latitude and longitude between weather data source and the simulation point [31]. The daily data from matched stations are then averaged using inverse distance as weights.

Future climate normals for the period 2021–2050 were obtained from daily output of the Canadian Centre for Climate Modelling and Analysis, Canadian Regional Model 4 [32], Canadian Earth System Model 2 [33], greenhouse gas concentration scenario RCP 4.5 [34]. Scenario RCP 4.5 is a middle-of-the-road, rather optimistic scenario, with a levelling off of greenhouse gas concentrations near the end of the 21st century. The forecast climate model output had 25 km horizontal resolution [35]. When using normals, BioSIM

generates stochastic daily values of minimum and maximum temperatures based on the monthly means, variances, auto- and cross-correlation information that constitute the normals [36,37].

The model was run for the Armagh and Epaule locations (open circles, Figure 2) in years for which parasitoid attack rate data were available. Because the model is stochastic, each run was replicated 10 times and output was averaged over replicates to provide adequate precision. We compared observed attack rates (the proportion of sentinel larvae successfully attacked by the parasitoids during successive 7-day exposures in the field), with the predicted frequency of the first generation adults. For this comparison, the maximum predicted frequency of adults was adjusted to match the maximum observed attack frequency on a location and year basis. The seasonality of *A. interrupta* is mostly unknown (but see [24]). To explore this question, we ran the integrated 3-species model for the Armagh and Epaule sites, from 1986 to 2019. Daily output was averaged over years for each location.

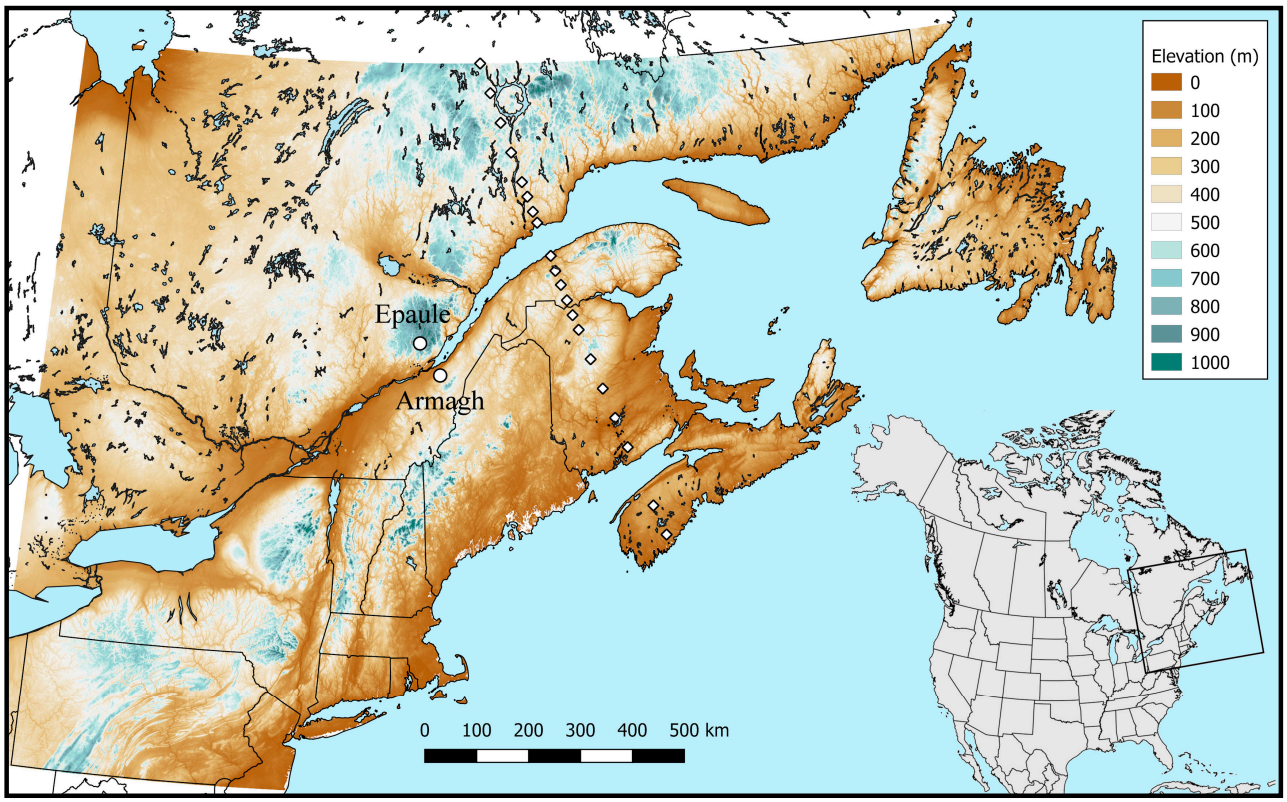

Figure 2. Elevation map of northeastern North America, illustrating the location of Armagh and Epaule sites (**open circles**), and of 20 locations along a latitudinal simulation transect (**diamonds**).

Maps of potential annual *A. interrupta* population growth rates were prepared by running the model for 20,000 randomly located simulation points over northeastern North America, between 39°30′ N by 81° W and 52° N by 52°30′ W. Two maps were prepared using observed weather over the periods 1961–1990 and 1991–2020 as input. A third map used normals (30 replicates of randomized daily values) for the period 2021–2050. The results were interpolated by universal kriging, using elevation as external drift variable. Elevations were obtained from a digital elevation model at 250 m horizontal resolution (Figure 2). To help interpret the mapping results, we averaged temperature over the period 1 May to 30 September at each simulation point for each 30-year period. We also calculated the average growth rate (number of overwintering progeny, all in OBL, divided by the 100 initial individuals) for each 30-year period. The relationships between the annual growth rate, mean summer temperature and latitude were graphed, for the three periods.

A series of simulations was run along a north-south transect of 20 locations (diamonds, Figure 2) between the northern edge of the Manicouagan Reservoir, QC (50° N, 69.57° W) and Little Lake, just north of Wilkins, NS (44° N, 65° W), using either 1991–2020 weather data or 2021–2050 climate normals. Each simulation was replicated 10 times, with 30 years of stochastically generated daily minimum and maximum air temperatures when using normals. Model output was summarized by generation (survival rate, fecundity, contribution to the end-of-season overwintering populations) for each location along the transect, for each period.

3. Results

3.1. Model Fitting

The parameter values of Equation (1) were obtained with a maximum-likelihood algorithm [6] (Table 1). Development times, rates, and the distribution of the individual variation term ε are very precisely described by this model (Figure 3). However, it should be noted that development at the lower end of the temperature range was not measured precisely and the value of the lower threshold temperature was set at $T_b = 0$ for the larval stages developing afterdiapause in OBL larvae. The lognormal distribution described quite well the observed distribution of individual deviations from the mean development time (Figure 3g–i).

Table 1. Parameter estimates for Equation (1) describing the developmental responses of *A. interrupta* to temperature, obtained from SAS procedure NLMIXED.

Parameter	Overwintered Maggot	Summer Maggot	Pupa
φ	0.0172 ± 0.0438	0.0561 ± 0.0256	0.0117 ± 0.0193
ω	0.0721 ± 0.7017	0.0513 ± 0.0295	0.1496 ± 0.0809
T_b	0 *	5.78 ± 0.31	1.78 ± 14.08
Δ_b	12.01 ±78.86	15.004 ± 10.00	5.05 ± 76.57
T_m	35.87 ± 3.73	33.37 ± 0.69	33.60 ± 0.97
Δ_m	11.09 ± 44.03	4.54 ± 1.80	5.87 ± 2.17
σ_ε	0.3031 ± 0.0292	0.1867 ± 0.0059	0.1237 ± 0.0062
MLH	−196.6	−1156.0	−470.0

* Parameter value fixed (not estimated).

3.2. Comparison of Model Output with Field Observations

The match between observed attack rates on sentinel larvae and predicted adult abundance was very good in Armagh (r = 0.88), less so at Epaule (r = 0.32, Figure 4).

The model predicted very well the date of the start of attacks in both locations (r = 0.83, Figure 5a), but did more poorly with the date of peak attack (r = 0.58), especially at Epaule (Figure 5b). The observed dates of first and peak attack were related, by general linear model, to location as a factor and predicted date as a covariate. The covariance with predicted dates was the only significant term for both first and peak dates of attack. The overall mean observed dates of onset of attack was not significantly different from predicted dates (171.3 ± 1.6 vs. 167.6 ± 1.3, t = 1.8, DF = 91, $p = 0.08$). However, the observed dates of peak attack were significantly earlier than the predicted dates of peak adult abundance (184.0 ± 1.2 vs. 191.9 ± 1.8, t = −3.7, df = 84, $p < 0.001$). The slope of the relationship between the observed date of first attack and the predicted date of first adults was not significantly different from 1 (F = 0.44, df = 1,45, $p = 0.51$). However, for the date of peak attack, this slope was considerably lower than 1 (F = 13.7, df = 1,45, $p = 0.001$). Thus, the observed attack period was shorter than expected from the predicted abundance of first generation adults. This was most pronounced at Epaule, where attack rates were later and much lower than in Armagh.

3.3. Predicted Seasonality in Armagh and at Epaule

The daily averaged model output indicated that in Armagh, the parasitoid can undergo four complete generations, while its OBL host undergoes three larval generations (Figure 6a). Adults of the overwintered generation are present from early June to late August, peaking in early July (Figure 6b). These adults are active during the latter half of the SBW's larval period, and while OBL larvae of the first generation are also present, as well as during the first half of the period of larval development of OBL's second generation. None of the progeny of these adults enter diapause in an OBL host. The adults of the first summer generation are active from mid-July to late September, peaking in mid-August (Figure 6c), and exploit the late-instar larvae of the OBL's second generation as well as early-instar larvae of the host's third generation (Figure 6a). Many of the parasitoids produced by this generation enter diapause (Figure 6d). The remainder develop to adults of the second summer generation, peaking in early September. Nearly all of the progeny of those second generation adults enter diapause in OBL larvae (Figure 6e). At Epaule, temperatures are much cooler (mean over 1986–2019: 11.07 ± 0.07 °C; days without frost: 129.9 ± 1.7 d) than in Armagh (mean over 1986–2019: 15.18 ± 0.07 °C; days without frost: 182.7 ± 1.1 d) because of the site's high elevation (789 m at Epaule compared to 277 m in Armagh). As a result, both OBL and *A. interrupta* undergo fewer generations at Epaule than in Armagh, with only two adult generations of *A. interrupta*. Late-instar SBW larvae and overwintered OBL larvae are attacked at the very beginning of the activity period of first generation parasitoid adults (Figure 6f,g). About 30% of the parasitoid population overwintering inside OBL larvae are issued from the first generation adults (Figure 6h). The remaining 70% are produced by second generation adults (Figure 6i). At Epaule, the progeny of second generation adults that develop in non-diapausing hosts do not reach the adult stage and therefore leave no progeny.

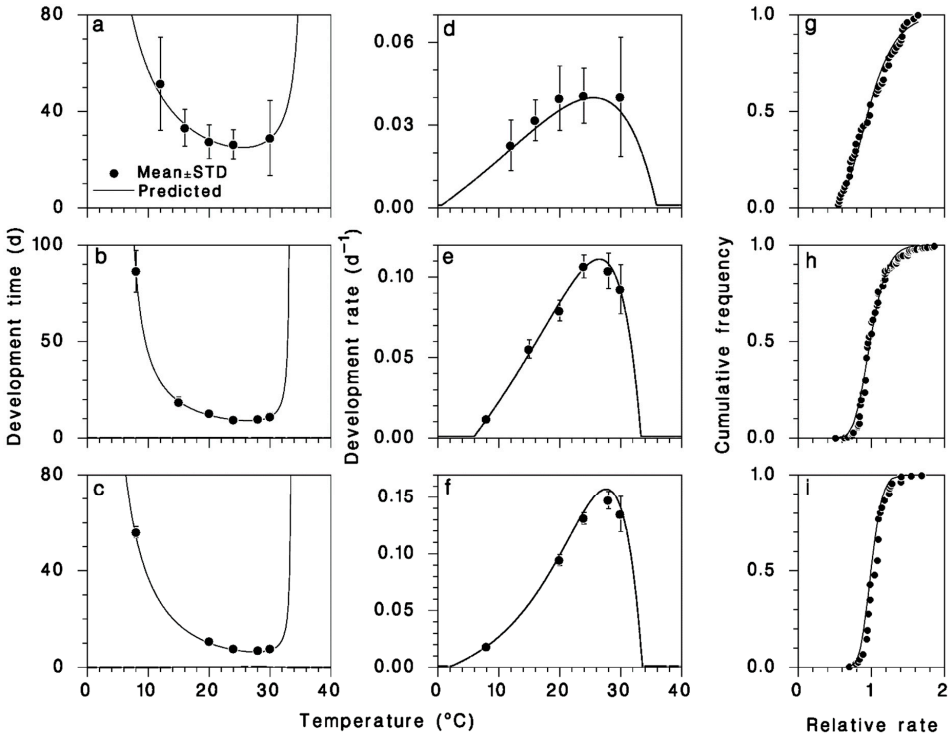

Figure 3. Relationship between *A. interrupta* development times (**a**–**c**), rates (**d**–**f**), and temperature. Points are means ± standard deviation. Distribution of individual values of ε compared to the lognormal (**g**–**i**).

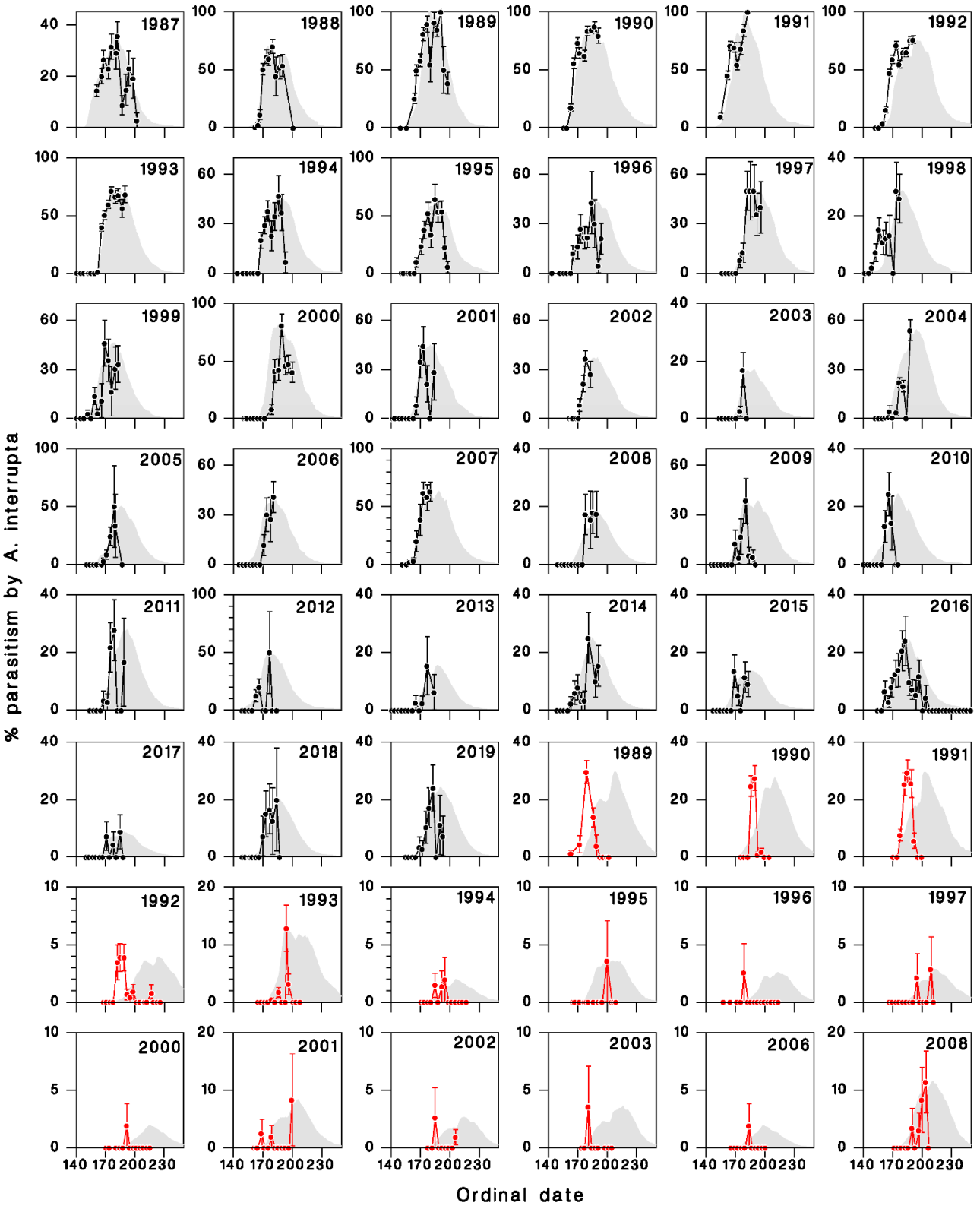

Figure 4. Comparison of attack rates on sentinel SBW larvae exposed in Armagh (•) and at Epaule (•), and predicted abundance of first-generation *A. interrupta* adults (**shaded curves**). Vertical bars are standard deviations ($\sqrt{pq/n}$) Note that the predicted adult abundance is adjusted so maximum observed and predicted values correspond.

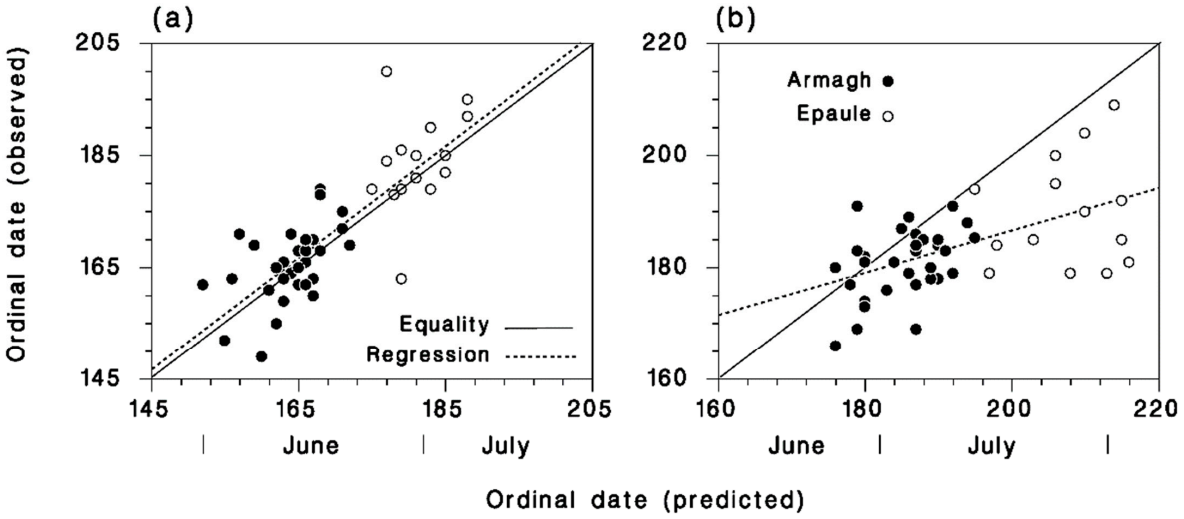

Figure 5. Comparison of the observed and predicted dates of (**a**) the start and (**b**) the peak of attacks on SBW larvae at Armagh (•) and Epaule (○). **Solid lines** are equality, **dotted lines** are regression. The difference between observed and predicted dates of the start of *A. interrupta* parasitism is 4.5 days, very close to our estimate of a 5-day pre-larviposition period.

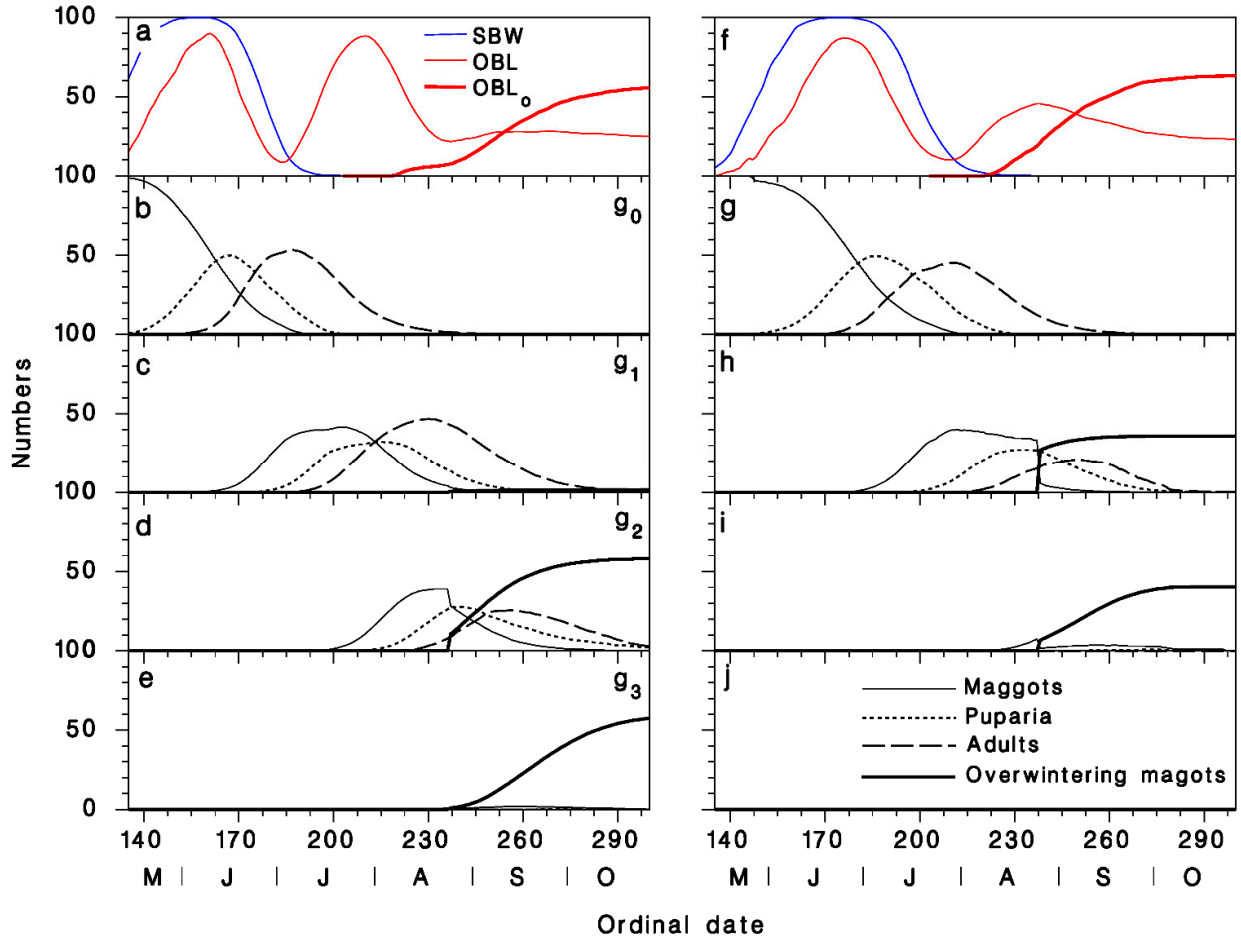

Figure 6. Model output in Armagh (**a**–**e**) and at Epaule (**f**–**j**), averaged over the period 1986–2019. (**a**,**f**) Abundance of larvae of the two hosts *C. fumiferana* (**blue**) and *C. rosaceana* (developing: **red**; in diapause: **bold red**); (**b**,**g**) overwintered generation of *A. interrupta*; (**c**,**h**) first summer generation; (**d**,**i**) second summer generation; (**e**,**j**) third summer generation. Maggots in hosts (**solid**), puparia on foliage (**dotted**), adults (**dashed**) and overwintering maggots (technically, part of the following generation; **bold**).

These simulations suggest that the potential growth rate of *A. interrupta* is, to a large extent, determined by the number of generations (all else being equal). In Armagh, the number of overwintering maggots produced by the initial 100 individuals averages 117 (thus annual growth rate $R = 1.17 \pm 0.05$, $n = 34$), while at Epaule, this number is 85 ($R = 0.85 \pm 0.05$, $n = 34$).

3.4. Spatial Simulation

3.4.1. Mapping

The maps of the *A. interrupta* population growth rate predicted by the model from past (from observed 1961–1990 weather, Figure 7a), current (from observed 1991–2020 weather, Figure 7b) and future climate (from normals for 2021–2050, Figure 7c) illustrate the profound impact of geography and climate change on the interaction between the parasitoid and its hosts. Under past and current climate, the parasitoid performed best at lower elevations over a band of latitudes in the range 45–49° N (Figure 7a,b). Under climate change, in the near future (2021–2050), the distribution of the highest population growth rates is expected to shift northward, and towards higher elevations (Figure 7c).

The average summer temperature from May to September over the 20,000 simulation points used to generate the maps in Figure 7, has increased from 13.91 ± 0.02 °C in 1961–1990 to 14.55 ± 0.02 °C in 1991–2020, and further to 16.67 ± 0.02 °C in 2021–2050 (Figure 8a). This warming seems to have advantaged *A. interrupta*, in terms of population growth rate. Mean annual growth rate R increased from 0.733 ± 0.002 during the period 1961–1990, to 0.799 ± 0.002 in 1991–2020, and is expected to remain virtually unchanged 0.8 ± 0.002 in the period 2021–2050, although optimal latitude will shift a full 2.5° N from 46 to 48.5° N over the 60-year period (Figure 8b). However, the expected population growth rate of the parasitoid exhibited a complex multimodal pattern, with maxima at 11, 16 and 21 °C (Figure 8c). This pattern was essentially the same in 1991–2020 as in 1961–1990. However, the growth rate maxima at 6 and 21 °C are expected to be more pronounced in 2021–2050 (blue symbols in Figure 8c).

3.4.2. Transect

The complex impact of latitude, elevation and climate change on the performance of the parasitoid can be better understood by examining the variations of survival and reproductive success of the parasitoid along the north-south transect of locations (diamonds in Figure 2). For this, the model output was summarized by generation (survival rate, realized fecundity, contribution to the end-of-season overwintering populations) along the transect, for each period (Figure 9). Survival in our model is mostly conditioned on the ability of the parasitoid to be in an overwintering host when frost occurs in late summer or early fall. This is a complex response to timing of each adult generation's progeny with entry of OBL larvae into diapause. Along our transect, higher mortality occurs at higher elevations and latitudes especially during the second and third summer parasitoid generations (Figure 9a,e). Fecundity, which is determined to a very large extent by the amount of overlap between parasitoid adult activity and the abundance of host larvae, is high in the first two adult generations, and drops sharply in the last two parasitoid generations at higher latitudes under current climate (Figure 9b). Under climate change, the fecundity of those two generations is actually higher at higher elevations along the middle of the transect, and drops at lower latitudes (Figure 9f). It is this pattern of realized fecundity that determines the spatial pattern of annual growth rates (Figure 9c,g). This explains the shift in optimum towards more northerly and higher-elevation locations. The relative contribution of each generation to the overwintering parasitoid population does not change much between the two temperature regimes (Figure 9d,e).

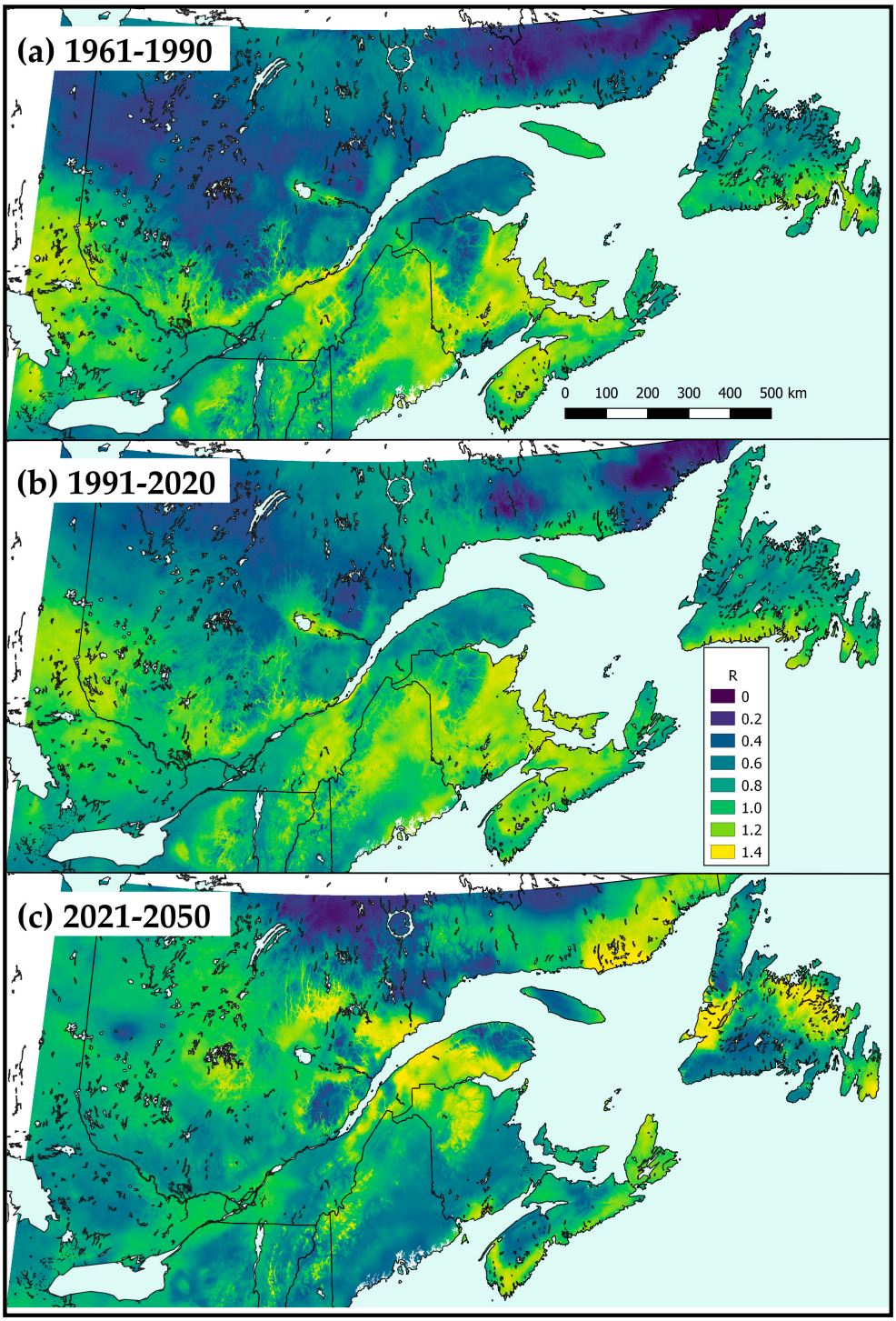

Figure 7. Maps of annual population growth rate of *Actia interrupta* over northeastern North America, using (**a**) observed 1961–1990 weather; (**b**) observed 1991–2020 weather; and (**c**) 2021–2050 randomized daily from normals of IPCC's greenhouse gas emission scenario RCP 4.5.

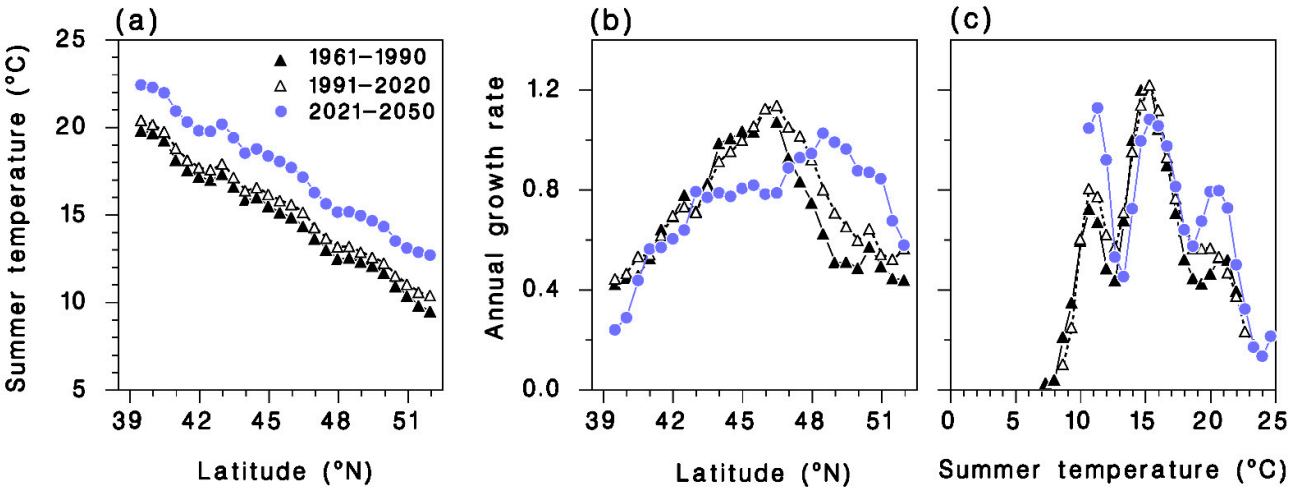

Figure 8. Relationship between latitude and (**a**) mean summer temperature from May to September and (**b**) average annual population growth rate of *Actia interrupta* compiled from 20,000 random locations in eastern North America. (**c**) Relationship between annual population growth rate and mean summer temperature. Model output from daily air temperature records 1961–1990 (▲), 1991–2020 (Δ), or from climate-changed disaggregated normals 2021–2050 (●).

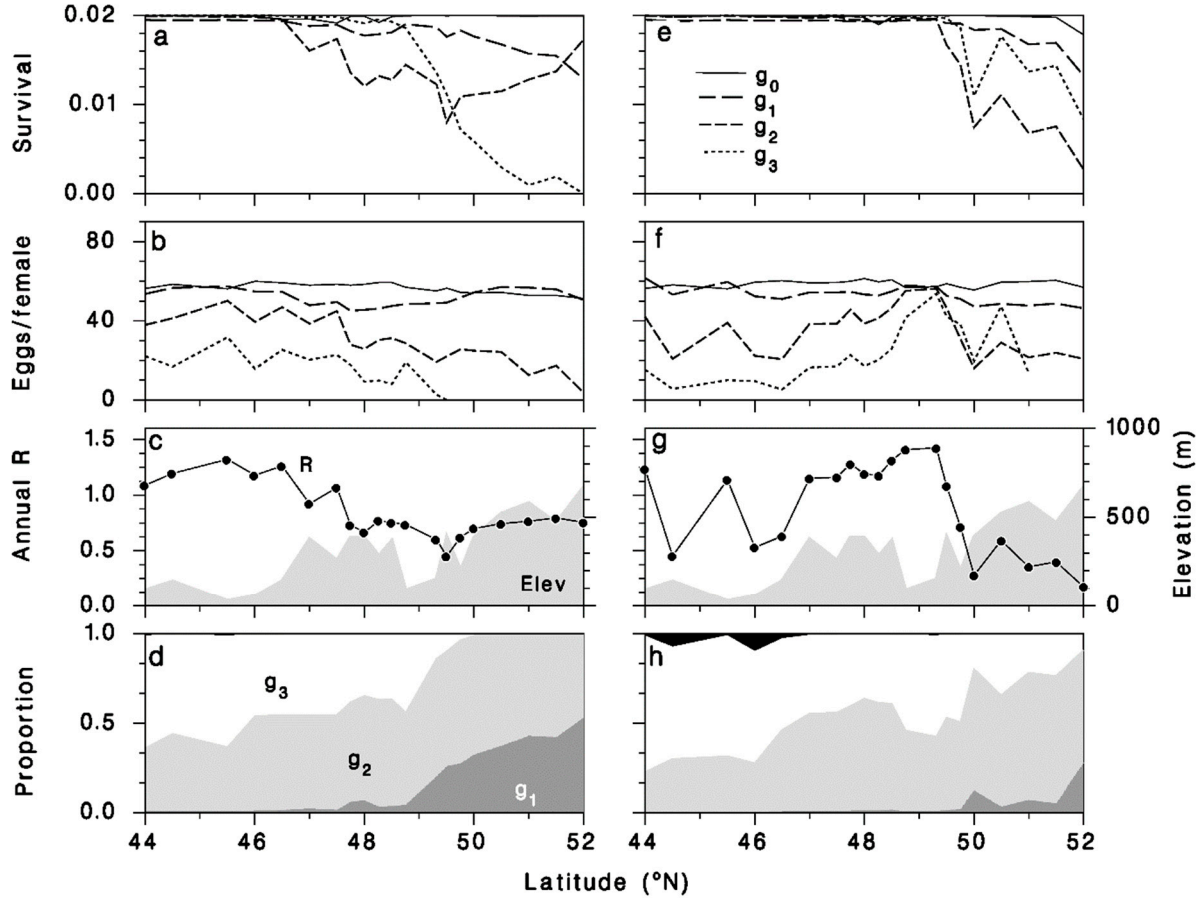

Figure 9. Model output along the latitudinal transect (diamonds in Figure 2) using weather from periods 1991–2020 (**a**–**d**) and 2021–2050 (**e**–**h**). (**a**,**e**) *Actia interrupta* survival from maggot to adult, including 97.96% culling in each generation. (**b**,**f**) Realized fecundity. (**c**,**g**) Annual population growth rate (overwintering maggots) and elevation (**gray shade**). (**d**,**h**) Contribution (proportion) of each generation of adults to the overwintering population. Initial generation (g_0: **solid**), subsequent generations (g_1: **long dash**, g_2: **short dash**, g_3: **dotted**).

4. Discussion

To better understand the seasonal biology of *Actia interrupta*, in particular as it pertains to synchrony between the adult fly and larvae of two of its major hosts in eastern conifer forests, the SBW and the OBL, we modeled the developmental responses to temperature of the parasitoid's three life stages: maggots inside the host, pupae and adults. From these responses, we developed an individual-based simulation model of the parasitoid's seasonal biology and linked it to phenology models for these two tortricid hosts [19,23]. The model initiates the parasitoid population as young larvae inside diapausing OBL larvae. The adults from that first parasitoid generation can then attack SBW larvae that are available as hosts only from mid-May to late June [23].

Our model shows that *A. interrupta* can have between two and four generations of adults per year, depending on local climate, and that in general the last adult generation is well timed with the diapause initiation in OBL larvae, allowing their progeny to spend winter in their larval host. The voltinism and overwintering strategy of *A. interrupta* make it clearly well adapted to the seasonal biology of its multivoltine OBL host, with two to three generations per year, depending on climatic conditions (Figure 6). In that context, it seems likely that SBW is not central in the parasitoid's life history strategy, and that its demographic impact on SBW may represent "collateral damage". SBW abundance may have an impact on the reproductive performance of the first generation of parasitoid adults, and could have a strong negative impact on the population growth rates of OBL. These dynamic aspects of the three species' interactions remain to be explored.

The equations describing the developmental responses of *A. interrupta* to temperature are reasonably accurate and provide good estimates of their variability at the individual level. Because development times below 8 °C were not observed, the predicted developmental responses near a probable lower threshold are poorly known (Table 1; Figure 3). Reproductive system development and output, host-searching behavior, and ageing are all temperature-dependent in adult parasitoids [19,38,39]. We also had no data to describe the temperature responses of adults, either in terms of longevity or fecundity. In our model we used temperature-independent constants that constitute individual traits assigned at random from appropriate distributions (from unpublished data). The model could readily accommodate refinements resulting from research to fill those gaps. Nevertheless, we believe the predictions obtained from the model are representative of the impact of weather on the ecological interactions between the parasitoid and these two alternate hosts.

The model output predicting the occurrence of adult *A. interrupta* compares very favorably with observations in Armagh, both in terms of onset and duration of the attack period (Figure 4). The model also predicts accurately the beginning of the attack period at Epaule (Figure 5a), but the duration of the attack period is much shorter than expected (Figure 5b). This was also the case with the predictions obtained from the two other parasitoid models in this series [19,20]. The difference in the observed duration of the attack period between Armagh and Epaule was not predicted by our model. The fit between model and observations in the case of *Tranosema rostrale* was also much better in Armagh than at Epaule [19]. This suggests the existence of additional factors. One such factor may be parasitoid movement between habitats in search of alternate hosts. Many of *A. interrupta*'s known hosts in eastern North America occur on deciduous host plants. It is likely that parasitoid females focus their search on the larvae of these alternate hosts as soon as natural SBW larvae become unavailable in late June. The Epaule stand is highly coniferous, and topographically complex [26]. It is possible that most of those alternate hosts are abundant in distinct habitat patches there. By contrast, the Armagh stand is more diverse, far simpler topographically, and alternate hosts may be found throughout the stand.

The expected potential population growth rates of the parasitoid are highly patterned geographically (Figure 7), due to a complex relationship with climatic conditions (Figure 8) that affect the synchrony of the parasitoid's last generation with the overwintering stage of OBL (Figure 6). Under climate change, we expect the area most suitable for the parasitoid

to shift northward and towards higher elevations, mostly because of decreases in successful contributions of the last generation to the overwintering population pool (Figure 9).

5. Conclusions

Among the many impacts of climate change on ecosystems [1], host−parasite interactions are very important because of their role in the regulation of host populations [2,10,40]. We have modeled the impact of climate change on the seasonal biology of the ichneumonid *Tranosema rostrale* [19], the braconid *Meteorus trachynotus* [20] and now the tachinid *Actia interrupta*. We have shown that these impacts on the spatial patterns of potential population performance are determined mostly by synchrony between parasitoid adults and the proportion of host larvae that enter diapause in late summer. In all three cases, our models are based solely on the thermal responses of the parasitoid and two of their major host species. All three models predict a shift of both hosts and parasitoids northward or to higher altitudes, as is expected in many systems [41] as a result of local phenological mismatch [10,42]. However, our models do not take into consideration other types of adaptations that may also occur over time, such as changes in life history strategy, thermal responses or behavior [40,43]. Such adaptations may have considerable impact after a long period, but are difficult to anticipate. For example, the overwintering strategy of all three parasitoids discussed in this series is to spend winter inside a diapausing host larva. It is unclear whether there is sufficient genetic plasticity in these species to change this strategy. Climate change may also, over the long term, lead to changes in the species composition of forest stands that would have an impact on the invertebrate fauna.

Another aspect that we have not considered is the extent to which these low-density parasitoids of SBW interact with each other. We know there is competition between *Actia interrupta* and the ichneumonid wasp *Tranosema rostrale* [24]. Interactions with the braconid *Meteorus trachynotus* or the eulophid ectoparasitoid *Elachertus cacoeciae* (Howard) [44], are unknown and worthy of investigation.

The probable change in distribution resulting from climate change may have more immediate implications for the dynamics of spruce budworm outbreaks and may help explain the recent change in the distribution of outbreak epicenters along the river valleys of the North Shore of the St Lawrence estuary [45]. While a broad analysis of the spatiotemporal patterns of population change in Quebec over the last 30 years failed to associate fluctuations of parasitism frequency in low-density SBW populations with outbreak development [46], evidence from rising SBW populations indicates that release from natural enemy pressure, including from parasitism, is involved in the spread of outbreaks [47].

Author Contributions: Conceptualization, J.R. and J.-C.T.; methodology, J.R., J.-C.T.; validation, J.R. and V.M.; formal analysis, J.R.; investigation, J.R., J.-C.T.; resources, J.R. and V.M.; data curation, J.R., J.-C.T. and V.M.; coding and implementation: R.S.-A.; writing—original draft preparation, J.R.; writing—review and editing, J.R., J.-C.T. and V.M.; visualization, J.R.; supervision, J.R. and V.M.; project administration, J.R. and V.M.; funding acquisition, J.R. and V.M. All authors have read and agreed to the published version of the manuscript.

Funding: This research was funded in part by members of SERG International, with contributions from the provincial governments of Newfoundland, Nova Scotia, New Brunswick, Quebec. Ontario, Manitoba, Saskatchewan, Alberta and British Columbia, as well as the USDA Forest Service.

Data Availability Statement: Data included in this study are available upon request from the corresponding author.

Acknowledgments: Thanks to the many people contributed to the collection of field data, in particular Pierre Duval. We thank especially the staff of the Ministère de la Faune, Forêts et Parcs du Québec, under the supervision of Pierre Therrien.

Conflicts of Interest: The authors declare no conflict of interest.

References

1. Malhi, Y.; Franklin, J.; Seddon, N.; Solan, M.; Turner, M.G.; Field, C.B.; Knowlton, N. Climate change and ecosystems: Threats, opportunities and solutions. *Philos. Trans. R. Soc. B Biol. Sci.* **2020**, *375*, 20190104. [CrossRef]
2. Chidawanyika, F.; Mudavanhu, P.; Nyamukondiwa, C. Global Climate Change as a Driver of Bottom-Up and Top-Down Factors in Agricultural Landscapes and the Fate of Host-Parasitoid Interactions. *Front. Ecol. Evol.* **2019**, *7*. [CrossRef]
3. Bouyer, J.; Cordier, S.; Levallois, P. Épidémiologie. In *Environnement et Santé Publique—Fondements et Pratiques*; Guérin, M., Gosselin, P., Cordier, S., Viau, C., Quénel, P., Dewailly, É., Eds.; Edisem: Acton Vale, QC, Canada, 2003; pp. 89–119. Available online: https://espum.umontreal.ca/lespum/departement-de-sante-environnementale-et-sante-au-travail/production-scientifique/livres/environnement-et-sante-publique-fondements-et-pratiques/ (accessed on 21 October 2021).
4. Bradshaw, C.J.A.; Leroy, B.; Bellard, C.; Roiz, D.; Albert, C.; Fournier, A.; Barbet-Massin, M.; Salles, J.-M.; Simard, F.; Courchamp, F. Massive yet grossly underestimated global costs of invasive insects. *Nat. Commun.* **2016**, *7*, 12986. [CrossRef]
5. Logan, J.A.; Régnière, J.; Powell, J.A. Assessing the impacts of global climate warming on forest pest dynamics. *Front. Ecol. Environ.* **2003**, *1*, 130–137. [CrossRef]
6. Régnière, J.; Powell, J.; Bentz, B.; Nealis, V. Effects of temperature on development, survival and reproduction of insects: Experimental design, data analysis and modeling. *J. Insect Physiol.* **2012**, *58*, 634–647. [CrossRef] [PubMed]
7. McManis, A.E.; Powell, J.A.; Bentz, B.J. Developmental parameters of a southern mountain pine beetle (Coleoptera: Curculionidae) population reveal potential source of latitudinal differences in generation time. *Can. Entomol.* **2018**, *151*, 1–15. [CrossRef]
8. Chuine, I.; Régnière, J. Process-Based Models of Phenology for Plants and Animals. *Annu. Rev. Ecol. Evol. Syst.* **2017**, *48*, 159–182. [CrossRef]
9. Schmitz, O.J.; Barton, B.T. Climate change effects on behavioral and physiological ecology of predator–prey interactions: Implications for conservation biological control. *Biol. Control.* **2014**, *75*, 87–96. [CrossRef]
10. Gehman, A.-L.M.; Hall, R.J.; Byers, J. Host and parasite thermal ecology jointly determine the effect of climate warming on epidemic dynamics. *Proc. Natl. Acad. Sci. USA* **2018**, *115*, 744–749. [CrossRef]
11. Laws, A.N. Climate change effects on predator–prey interactions. *Curr. Opin. Insect Sci.* **2017**, *23*, 28–34. [CrossRef]
12. Daugaard, U.; Petchey, O.L.; Pennekamp, F. Warming can destabilize predator–prey interactions by shifting the functional response from Type III to Type II. *J. Anim. Ecol.* **2019**, *88*, 1575–1586. [CrossRef]
13. Johnston, A.S.A.; Boyd, R.J.; Watson, J.W.; Paul, A.; Evans, L.C.; Gardner, E.L.; Boult, V.L. Predicting population responses to environmental change from individual-level mechanisms: Towards a standardized mechanistic approach. *Proc. R. Soc. B Boil. Sci.* **2019**, *286*, 20191916. [CrossRef]
14. Johns, R.; Bowden, J.; Carleton, R.D.; Cooke, B.J.; Edwards, S.; Emilson, E.; James, P.M.A.; Kneeshaw, D.; MacLean, D.A.; Martel, V.; et al. A conceptual framework for the spruce budworm early intervention strategy: Can outbreaks be stopped? *Forests* **2019**, *10*, 910. [CrossRef]
15. Boulanger, Y.; Arseneault, D. Spruce budworm outbreaks in eastern Quebec over the last 450 years. *Can. J. For. Res.* **2004**, *34*, 1035–1043. [CrossRef]
16. Boulanger, Y.; Arseneault, D.; Morin, H.; Jardon, Y.; Bertrand, P.; Dagneau, C. Dendrochronological reconstruction of spruce budworm (*Choristoneura fumiferana*) outbreaks in southern Quebec for the last 400 years1This article is one of a selection of papers from the 7th International Conference on Disturbance Dynamics in Boreal Forests. *Can. J. For. Res.* **2012**, *42*, 1264–1276. [CrossRef]
17. Eveleigh, E.S.; McCann, K.S.; McCarthy, P.C.; Pollock, S.J.; Lucarotti, C.J.; Morin, B.; McDougall, G.A.; Strongman, D.B.; Huber, J.T.; Umbanhowar, J.; et al. Fluctuations in density of an outbreak species drive diversity cascades in food webs. *Proc. Natl. Acad. Sci. USA* **2007**, *104*, 16976–16981. [CrossRef]
18. Greyson-Gaito, C.J.; McCann, K.S.; Fründ, J.; Lucarotti, C.J.; Smith, M.A.; Eveleigh, E.S. Parasitoid community responds indiscriminately to fluctuating spruce budworm (Lepidoptera: Tortricidae) and other caterpillars on balsam fir (Pinaceae). *Can. Entomol.* **2021**, *153*, 482–496. [CrossRef]
19. Régnière, J.; Seehausen, M.L.; Martel, V. Modeling climatic influences on three parasitoids of low-density spruce budworm populations. Part 1: Tranosema rostrale (Hymenoptera: Ichneumonidae). *Forests* **2020**, *11*, 846. [CrossRef]
20. Régnière, J.; Saint-Amant, R.; Thireau, J.-C.; Therrien, P.; Hébert, C.; Martel, V. Modeling Climatic Influences on Three Parasitoids of Low-Density Spruce Budworm Populations. Part 2: *Meteorus trachynotus* (Hymenoptera: Braconidae). *Forests* **2021**, *12*, 155. [CrossRef]
21. Arnaud, P.H. *A Host-Parasite Catalog of North American Tachinidae (Diptera)*; U.S. Department of Agriculture, Miscellaneous Publication: Washington, DC, USA, 1978. Available online: https://archive.org/details/hostparasitecata1319arna (accessed on 21 October 2021).
22. O'Hara, J.E. Revision of nearctic species ofactiarobineau-desvoidy (diptera: Tachinidae). *Can. Entomol.* **1991**, *123*, 745–776. [CrossRef]
23. Régnière, J.; St-Amant, R.; Duval, P. Predicting insect distributions under climate change from physiological responses: Spruce budworm as an example. *Biol. Invasions* **2010**, *14*, 1571–1586. [CrossRef]
24. Cusson, M.; LaForge, M.; Régnière, J.; Béliveau, C.; Trudel, D.; Thireau, J.-C.; Bellemare, G.; Keirstead, N.; Stolz, D. Multiparasitism of *Choristoneura fumiferana* by the ichneumonid Tranosema rostrale and the tachinid Actia interrupta: Occurrence in the field and outcome of competition under laboratory conditions. *Entomol. Exp. Appl.* **2002**, *102*, 125–133. [CrossRef]

25. Martel, V.; Thireau, J.-C.; Régnière, J. Manual inoculation of host larvae with first instar maggots as a rearing technique for the larval parasitoid *Actia interrupta* (Diptera: Tachinidae). *Biocontrol Sci. Technol.* **2021**, 1–4. [CrossRef]
26. Lethiecq, J.L.; Régnière, J. *CFS Spruce Budworm Population Studies: Sites Descriptions*; Info. Rep. LAU-X-83; Canadian Forest Service, Laurentian Forestry Centre: Quebec, QC, Canada, 1988. Available online: https://cfs.nrcan.gc.ca/publications/download-pdf/21262 (accessed on 21 October 2021).
27. Seehausen, M.L.; Régnière, J.; Martel, V.; Smith, S.M. Seasonal Parasitism and Host Instar Preference by the Spruce Budworm (Lepidoptera: Tortricidae) Larval Parasitoid *Tranosema rostrale* (Hymenoptera: Ichneumonidae). *Environ. Entomol.* **2016**, *45*, 1123–1130. [CrossRef]
28. Régnière, J.; St-Amant, R.; Béchard, A. *BioSIM 10—User's Manual*; Info. Rep. LAU-X-155; Canadian Forest Service, Laurentian Forestry Centre: Quebec, QC, Canada, 2014. Available online: https://cfs.nrcan.gc.ca/publications/download-pdf/34818 (accessed on 21 October 2021).
29. Gangavalli, R.; Aliniazee, M. Diapause induction in the oblique-banded leafroller *Choristoneura rosaceana* (Lepidoptera: Tortricidae): Role of photoperiod and temperature. *J. Insect Physiol.* **1985**, *31*, 831–835. [CrossRef]
30. Holling, C.S. Some Characteristics of Simple Types of Predation and Parasitism. *Can. Entomol.* **1959**, *91*, 385–398. [CrossRef]
31. Régnière, J. Generalized Approach to Landscape-Wide Seasonal Forecasting with Temperature-Driven Simulation Models. *Environ. Entomol.* **1996**, *25*, 869–881. [CrossRef]
32. Scinocca, J.F.; Kharin, V.V.; Jiao, Y.; Qian, M.W.; Lazare, M.; Solheim, L.; Flato, G.M.; Biner, S.; Desgagne, M.; Dugas, B. Coordinated Global and Regional Climate Modeling. *J. Clim.* **2015**, *29*, 17–35. [CrossRef]
33. Arora, V.K.; Scinocca, J.F.; Boer, G.J.; Christian, J.R.; Denman, K.L.; Flato, G.M.; Kharin, V.V.; Lee, W.; Merryfield, W.J. Carbon emission limits required to satisfy future representative concentration pathways of greenhouse gases. *Geophys. Res. Lett.* **2011**, *38*. [CrossRef]
34. Pachauri, R.K.; Allen, M.R.; Barros, V.R.; Broome, J.; Cramer, W.; Christ, R.; Church, J.A.; Clarke, L.; Dahe, Q.; Dasgupta, P.; et al. *Contribution of Working Groups I, II and III to the Fifth Assessment Report of the Intergovernmental Panel on Climate Change*; Climate Change 2014: Synthesis Report; IPCC: Geneva, Switzerland, 2014; p. 151. Available online: https://www.ipcc.ch/report/ar5/syr (accessed on 21 October 2021).
35. Canadian Centre for Climate Modelling and Analysis (CCCma) Climate Model Data, CanESM2/CGCM4 Model Output. 2018. Available online: http://climate-modelling.canada.ca/climatemodeldata/cgcm4/CanESM2/rcp45/ (accessed on 21 October 2021).
36. Régnière, J.; Bolstad, P. Statistical Simulation of Daily Air Temperature Patterns Eastern North America to Forecast Seasonal Events in Insect Pest Management. *Environ. Entomol.* **1994**, *23*, 1368–1380. [CrossRef]
37. Régnière, J.; St-Amant, R. Stochastic simulation of daily air temperature and precipitation from monthly normals in North America north of Mexico. *Int. J. Biometeorol.* **2007**, *51*, 415–430. [CrossRef]
38. Seehausen, M.L.; Régnière, J.; Martel, V.; Smith, S.M. Developmental and reproductive responses of the spruce budworm (Lepidoptera: Tortricidae) parasitoid *Tranosema rostrale* (Hymenoptera: Ichneumonidae) to temperature. *J. Insect Physiol.* **2017**, *98*, 38–46. [CrossRef]
39. Lauzière, I.; Setamou, M.; Legaspi, J.; Jones, W. Effect of Temperature on the Life Cycle of *Lydella jalisco* (Diptera: Tachinidae), a Parasitoid of *Eoreuma loftini* (Lepidoptera: Pyralidae). *Environ. Entomol.* **2002**, *31*, 432–437. [CrossRef]
40. Harvey, J.A. Conserving host–parasitoid interactions in a warming world. *Curr. Opin. Insect Sci.* **2015**, *12*, 79–85. [CrossRef]
41. Jeffs, C.T.; Lewis, O.T. Effects of climate warming on host-parasitoid interactions. *Ecol. Entomol.* **2013**, *38*, 209–218. [CrossRef]
42. Durant, J.M.; Molinero, J.-C.; Ottersen, G.; Reygondeau, G.; Stige, L.C.; Langangen. Contrasting effects of rising temperatures on trophic interactions in marine ecosystems. *Sci. Rep.* **2019**, *9*, 1–9. [CrossRef] [PubMed]
43. Tougeron, K.; Brodeur, J.; Le Lann, C.; van Baaren, J. How climate change affects the seasonal ecology of insect parasitoids. *Ecol. Entomol.* **2019**, *45*, 167–181. [CrossRef]
44. Fidgen, J.G.; Eveleigh, E.S. Life history characteristics of *Elachertus cacoeciae* (hymenoptera: Eulophidae), an ectoparasitoid of spruce budwor larvae, *Choristoneura fumiferana* (lepidoptera: Tortricidae). *Can. Entomol.* **1998**, *130*, 215–229. [CrossRef]
45. Bouchard, M.; Auger, I. Influence of environmental factors and spatio-temporal covariates during the initial development of a spruce budworm outbreak. *Landsc. Ecol.* **2013**, *29*, 111–126. [CrossRef]
46. Bouchard, M.; Martel, V.; Régnière, J.; Therrien, P.; Correia, D.L.P. Do natural enemies explain fluctuations in low-density spruce budworm populations? *Ecology* **2018**, *99*, 2047–2057. [CrossRef]
47. Régnière, J.; Cooke, B.J.; Béchard, A.; Dupont, A.; Therrien, P. Dynamics and Management of Rising Outbreak Spruce Budworm Populations. *Forests* **2019**, *10*, 748. [CrossRef]